Long noncoding miRNA gene represses wheat β-diketone waxes

Daiqing Huang[a,1], J. Allan Feurtado[a,1], Mark A. Smith[a], Leah K. Flatman[a], Chushin Koh[a,2], and Adrian J. Cutler[a,3]

[a]Wheat Improvement Flagship Program, National Research Council of Canada, Saskatoon, Saskatchewan, SK S7N 0W9, Canada

Edited by David C. Baulcombe, University of Cambridge, Cambridge, United Kingdom, and approved March 7, 2017 (received for review November 9, 2016)

The cuticle of terrestrial plants functions as a protective barrier against many biotic and abiotic stresses. In wheat and other Triticeae, β-diketone waxes are major components of the epicuticular layer leading to the bluish-white glaucous trait in reproductive-age plants. Glaucousness in durum wheat is controlled by a metabolic gene cluster at the *WAX1* (*W1*) locus and a dominant suppressor *INHIBITOR of WAX1* (*Iw1*) on chromosome 2B. The wheat D subgenome from progenitor *Aegilops tauschii* contains *W2* and *Iw2* paralogs on chromosome 2D. Here we identify the *Iw1* gene from durum wheat and demonstrate the unique regulatory mechanism by which *Iw1* acts to suppress a carboxylesterase-like protein gene, *W1-COE*, within the *W1* multigene locus. *Iw1* is a long noncoding RNA (lncRNA) containing an inverted repeat (IR) with >80% identity to *W1-COE*. The *Iw1* transcript forms a miRNA precursor-like long hairpin producing a 21-nt predominant miRNA, miRW1, and smaller numbers of related sRNAs associated with the nonglaucous phenotype. When *Iw1* was introduced into glaucous bread wheat, miRW1 accumulated, *W1-COE* and its paralog *W2-COE* were down-regulated, and the phenotype was nonglaucous and β-diketone–depleted. The IR region of *Iw1* has >94% identity to an IR region on chromosome 2 in *Ae. tauschii* that also produces miRW1 and lies within the marker-based location of *Iw2*. We propose the *Iw* loci arose from an inverted duplication of *W1-COE* and/or *W2-COE* in ancestral wheat to form evolutionarily young miRNA genes that act to repress the glaucous trait.

glaucous | inhibitor of wax | small RNA | long noncoding RNA | *WAX1*

Plant epicuticular waxes deposited on the outer surface of the plant cuticle produce a water-resistant layer that serves to reduce nonstomatal water loss and mitigate the effects of heat and UV radiation as well as pathogen and insect attacks (1). Grasses in the Triticeae tribe, subfamily Pooideae, which include the cultivated species barley (*Hordeum vulgare*; $2n = 2x = 14$), rye (*Secale cereale*, $2n = 2x = 14$), durum wheat (*Triticum durum*; $2n = 4x = 28$, AABB), and bread wheat (*Triticum aestivum*; $2n = 6x = 42$, AABBDD), have two predominant pathways for wax production: (*i*) an alcohol- and alkane-rich wax pathway and (*ii*) a pathway leading to β-diketones and derivatives including hydroxy-β-diketones (2). The alcohol and alkane waxes are prevalent in earlier development and on leaves, whereas β-diketones dominate during the reproductive phase, particularly on leaf sheaths and flower heads (3, 4). β-Diketone wax is predominantly hentriacontane-14, 16-dione, which consists of a 31-carbon chain with carbonyl groups at C_{14} and C_{16}. In durum wheat, about 20% of the β-diketone is hydroxylated to form 25-hydroxy-β-diketone, whereas in bread wheat hydroxylation is at C_8 or C_9 (5). β-Diketone wax deposition manifests visibly as glaucousness, a bluish-white coloration on stems, leaves, and flower heads. However, the relationship between a glaucous appearance and the total amount of cuticular wax can be inconsistent, especially during the later stages of wheat reproductive development (6, 7). Nonetheless, β-diketones are essential for the appearance of glaucousness and associated wax morphology (3). β-Diketone wax deposition and the development of glaucousness lead to a greater reflectance of incident light. Reduced light absorption can lower tissue temperatures, thereby reducing transpirational water loss, and also may reduce photosynthesis under nonsaturating illumination (1). In wheat, a glaucous appearance has been shown to be associated with stabilizing grain yield, particularly in growth environments that are water-limited and prone to heat stress (6, 8, 9). Thus, because of the protective nature of the waxy β-diketone layer, the glaucous appearance has generally been selected for during the breeding of cultivated durum and bread wheat varieties (3, 10). In contrast, a nonglaucous (NG) state is prevalent in the uncultivated relatives of wheat, including progenitor species wild emmer (*Triticum dicoccoides*, $2n = 4x = 28$, AABB) and *Aegilops tauschii* ($2n = 2x = 14$, DD) (11, 12). As such, these species have been used in the development of NG wheat varieties and for studies on the characterization of the genes and genetic loci involved in wax deposition, in particular *W1*/*W2* and *Iw1*/*Iw2* (13, 14).

The complex evolution of durum and bread wheat as multilevel genome mosaics means each of the three subgenomes in wheat (A, B, and D) has the potential to contribute to the inheritance of glaucousness (15). However, only the B and D subgenomes contain major glaucousness loci, and the A genome progenitor *Triticum urartu* does not contain any appreciable β-diketones and is NG (5, 16). Within the B subgenome, *WAX1* (*W1*) and *INHIBITOR OF WAX1* (*Iw1*) have been mapped very close to each other on the distal end of 2BS. Conversely, in the D subgenome, *W2* and *Iw2* have been mapped far apart, with *W2* at the proximal end and *Iw2* at the distal end of 2DS (16). As the name suggests, the *Iw* loci

Significance

Higher plants have waxy surface layers that prevent uncontrolled water loss. Many wheat cultivars accumulate diketone epicuticular waxes in reproductive-age plants that produce a glaucous appearance. We identify *INHIBITOR of WAX1* (*Iw1*), a dominant glaucous repressor, as a young miRNA gene (MIRNA) that produces an miRNA, miRW1, which targets the transcript of the biosynthetic gene *WAX1-CARBOXYLESTERASE* (*W1-COE*) for degradation. The high sequence similarity between the *Iw1* hairpin sequence and *W1-COE* suggests that this MIRNA gene arose from an inverted duplication of its target. The cleavage specificity of miRW1 for its target gene defines the unique role of a young MIRNA gene in the regulation of an important agricultural trait related to stress tolerance.

Author contributions: D.H., J.A.F., and A.J.C. designed research; D.H., J.A.F., M.A.S., and L.K.F. performed research; D.H., J.A.F., M.A.S., and C.K. analyzed data; and D.H., J.A.F., and A.J.C. wrote the paper.

The authors declare no conflict of interest.

This article is a PNAS Direct Submission.

Data deposition: The small RNA and RNA-sequencing data have been submitted to the Sequence Read Archive (SRA) at the National Center for Biotechnology Information (NCBI) [accession nos. SAMN05725181–SAMN05725246 (mRNAs and sRNA in *Triticum durum* and *Triticum aestivum*)]. The Iw1 full-length cDNA sequence was submitted to the NCBI expressed sequence tags database (dbEST) (accession no. KX823910).

[1]D.H. and J.A.F. contributed equally to this work.

[2]Present address: Global Institute for Food Security, University of Saskatchewan, Saskatoon, SK S7N 4J8, Canada.

[3]To whom correspondence should be addressed. Email: adrian.cutler@nrc-cnrc.gc.ca.

This article contains supporting information online at www.pnas.org/lookup/suppl/doi:10.1073/pnas.1617483114/-/DCSupplemental.

provide epistatic dominant inhibition over the *W* loci. In recent years, several reports have furthered the characterization of these loci, including fine-mapping of *Iw1* (11), demonstrating *Iw1* suppression of β-diketone wax accumulation (17), fine mapping of *Iw2* in *Ae. tauschii* (12), comparative mapping of *Iw1* and *Iw2* in hexaploid wheat (18), determining the impact of *W* and *Iw* loci on glaucousness and cuticle permeability (3), and fine mapping of *W1* in hexaploid wheat (19). The synthesis and chemistry of diketone waxes has been studied extensively in barley, chiefly through the characterization of loss-of-function mutants of three tightly linked loci collectively referred to as "*Cer-cqu*" (2, 20, 21). The *Cer-cqu* operon, as it has been described, is associated with the cer-c, -q, and -u complementation groups and corresponding mutants *glossy sheath 6* (*gsh6*), *gsh1*, and *gsh8*, respectively, and have been mapped close to the terminus of the short arm of chromosome 2H (22). A recent study identified the CER gene cluster including *GSH1* (*Cer-Q*) as encoding a lipase/carboxylesterase, *GSH6* (*Cer-C*), as a chalcone synthase-like polyketide synthase and *GSH8* (*Cer-U*) as a cytochrome P450-type hydroxylase (23). More recently, the wheat *W1* locus was identified as a gene cluster that is collinear to the barley CER gene cluster (24) and includes orthologs of *Cer-Q*, *Cer-C*, and *Cer-U* (23), which we define as W1-COE (carboxylesterase), W1-PKS (polyketide synthase), and W1-CYP (cytochrome P450 hydroxylase), respectively. However, it is not known which of the genes at the *W1* locus are regulated by *Iw1* and therefore are responsible for the presence or absence of diketone waxes and the glaucous phenotype. More importantly, the inhibitor genes *Iw1* and *Iw2* have not been identified, and their mechanism of action is unknown.

Long noncoding RNAs (lncRNAs) are a large and diverse class of RNA transcripts with a length of more than 200 nt that do not encode proteins. LncRNAs are emerging as important regulators in a wide range of essential biological processes. In humans, lncRNAs represent more than 68% of the transcriptome, and 79% of the lncRNAs were previously unannotated (25). Our current knowledge of their biological functions is limited, and lncRNA research in plants lags behind lncRNA research in animals. To date, very few lncRNAs have been characterized in detail (26). Some lncRNAs can be precursors of small RNAs (sRNAs) including miRNAs, which are a class of sRNA ranging from 20–24 nt in length that regulate numerous pathways and biological processes (27). miRNAs play significant roles in posttranscriptional gene regulation through base pairing with specific target sequences in their complementary mRNA targets, leading to transcript degradation (28, 29). The mechanism of action of miRNAs implies that they typically act as genetically dominant-negative regulators. Therefore, because the *Iw* loci are dominant repressors of the glaucous trait, we investigated the possible involvement of sRNAs in the regulation of wax accumulation. Using near-isogenic lines (NILS) from durum wheat that differed in glaucousness (30, 31), we compared the sRNAs in each of the isogenic pairs and identified a set of related miRNAs associated with repression of β-diketone deposition. We show that the *Iw1* locus is a miRNA gene (MIRNA) that encodes a miRNA precursor and represses β-diketone deposition via miRNA-mediated cleavage of *W1-COE* transcripts.

Results

To investigate the genetic basis for glaucousness in wheat, we characterized four pairs of NILs of durum wheat, AG1, AG2, AE3, and D051, defined by the presence or absence of the glaucous trait (30, 31). These lines were produced by back-crossing a NG cultivar to a glaucous parent and then maintaining heterozygosity for glaucousness in the F4 and later generations (*SI Appendix*, Table S1*A*) (31). Glaucous lines showed bluish-white coloration from the booting stage in the stems, leaves, and floral tissues, whereas NG lines were green and glossy (Fig. 1*A*). The cuticular wax content and composition from leaf sheaths of all four NIL pairs was analyzed by GC-MS. Glaucous lines contained primarily β-diketone (hentriacontane-14, 16-dione) and 25-hydroxy-β-diketone (25-hydroxyhentriacontane-14, 16-dione) (5, 32), whereas the NG lines contained no detectable diketone waxes (Fig. 1*B* and *SI Appendix*, Table S1). Importantly, crosses between three pairs of NILs, AG1, AG2, and AE3 (glaucous × NG), resulted in F1 plants that were 100% NG (*SI Appendix*, Fig. S1), confirming the dominance of the NG trait, as observed previously (30, 31).

Transcripts Associated with Wax Production in the Durum NILs. Transcripts in NIL pairs were compared to identify differences that were consistently associated with the loss of diketone wax production and glaucousness. Potential wax-related genes that were strongly down-regulated in NG lines were first identified by mapping reads to the National Center for Biotechnology Information (NCBI) unigene set and determining significant differences based on count data (edgeR, $P \leq 0.05$). We found 16 unigenes that were commonly down-regulated in all four glaucous/NG NIL comparisons (Dataset S1). Consistent with previous mapping studies locating *W1* and *Iw1* on 2BS (16), blasting the 16 unigenes against the International Wheat Genome Sequencing Consortium (IWGSC) wheat survey sequences from AABB genomes revealed that most of the contigs were located on 2BS scaffolds (Dataset S1). Through further bioinformatics analyses, we defined these 16 unigenes into seven potential target genes (Dataset S1). Three of these target genes, targets 1, 2, and 4, were from the *W1* locus gene cluster: *W1-COE*, *W1-PKS*, and *W1-CYP*. To confirm the significance of the differentially expressed genes from the NCBI unigene reference, we also used the IWGSC transcript set (v1 from EnsemblPlants) as a reference for analysis with the addition of the unannotated *W1-COE* sequence. Using this reference, the RNA sequencing (RNA-seq) data were reanalyzed using the pseudoalignment program kallisto and the Bioconductor package DESeq2 (adjusted *P* value ≤ 0.05) (33, 34). Similar differentially expressed target genes were obtained and included the W1 gene cluster: *W1-COE*, *W1-CYP* (*Traes_2BS_163390FC4*), target 6 (*Traes_2BS_D6F1011EA*), and *W1-PKS* (*Traes_2BS_9E10D26DB*) on 2BS and transcripts with high homology to *W1-PKS*: *Traes_3B_FC275A64D*, *Traes_4BS_AB8E1AD32*, and *Traes_6BS_C400F1983* (Dataset S2). With respect to expression level, all seven of the potential target genes showed virtually no expression in NG NILs with an average down-regulation of more than 2,800-fold (Fig. 1*C*). In F1 heterozygous lines, *W1-COE* expression was still down-regulated by 31.3-fold on average, but the expression of all other targets, including *W1-PKS* and *W1-CYP*, recovered to a large extent, showing down-regulation between 1.7- and 4.7-fold (Fig. 1*C*), suggesting that *W1-COE* is most likely the gene controlling the glaucous trait in these durum NILs.

To establish whether *W1-COE* is indeed involved in diketone wax production, we used virus-induced gene silencing (VIGS) to block its expression transiently in wheat. Fragments of *W1-COE* were integrated into a VIGS system using the barley stripe mosaic virus (35) and were applied to the leaves of glaucous AG2 plants at the tillering stage, before visible glaucousness was apparent. Then the development of glaucousness was monitored for 4–6 wk. *W1-COE* fragments all produced large reductions in visible glaucousness relative to waxy controls (*SI Appendix*, Fig. S2) and in total diketone wax accumulation in leaf sheaths (*SI Appendix*, Figs. S3*A* and S4). Control infections with a *PHYTOENE DESATURASE* (*PDS*) fragment produced a slight reduction in wax content which may be attributed both to the general effects of viral infection and to the reduction in pigment accumulation resulting from the inhibition of *PDS*. The levels of *W1-COE* expression in VIGS-treated plants were measured by quantitative PCR (qPCR), which showed that all four of the tested fragments reduced the expression of the gene (*SI Appendix*, Fig. S3*B*). In addition, there was a linear correlation between the amount of β-diketone wax and the expression of *W1-COE* (*SI Appendix*, Fig. S3*C*). The VIGS

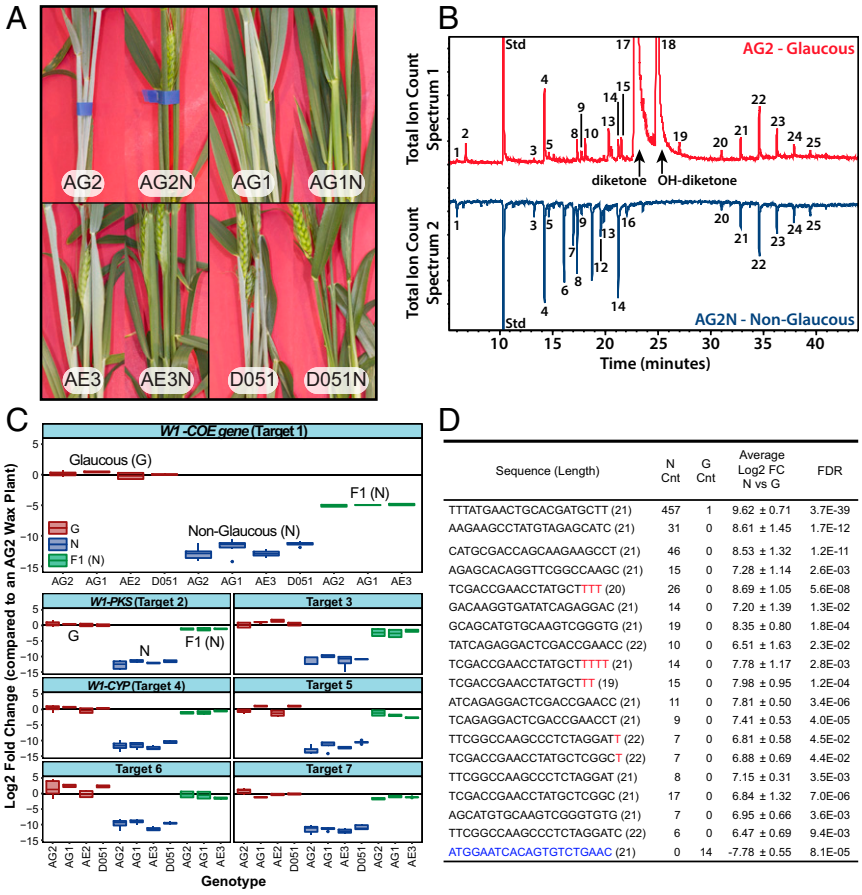

Sequence (Length)	N Cnt	G Cnt	Average Log2 FC N vs G	FDR
TTTATGAACTGCACGATGCTT (21)	457	1	9.62 ± 0.71	3.7E-39
AAGAAGCCTATGTAGAGCATC (21)	31	0	8.61 ± 1.45	1.7E-12
CATGCGACCAGCAAGAAGCCT (21)	46	0	8.53 ± 1.32	1.2E-11
AGAGCACAGGTTCGGCCAAGC (21)	15	0	7.28 ± 1.14	2.6E-03
TCGACCGAACCTATGCTTTT (20)	26	0	8.69 ± 1.05	5.6E-08
GACAAGGTGATATCAGAGGAC (21)	14	0	7.20 ± 1.39	1.3E-02
GCAGCATGTGCAAGTCGGGTG (21)	19	0	8.35 ± 0.80	1.8E-04
TATCAGAGGACTCGACCGAACC (22)	10	0	6.51 ± 1.63	2.3E-02
TCGACCGAACCTATGCTTTTT (21)	14	0	7.78 ± 1.17	2.8E-03
TCGACCGAACCTATGCTTT (19)	15	0	7.98 ± 0.95	1.2E-04
ATCAGAGGACTCGACCGAACC (21)	11	0	7.81 ± 0.50	3.4E-06
TCAGAGGACTCGACCGAACCT (21)	9	0	7.41 ± 0.53	4.0E-05
TTCGGCCAAGCCCTCTAGGATT (22)	7	0	6.81 ± 0.58	4.5E-02
TCGACCGAACCTATGCTCGGCT (22)	7	0	6.88 ± 0.69	4.4E-02
TTCGGCCAAGCCCTCTAGGAT (21)	8	0	7.15 ± 0.31	3.5E-03
TCGACCGAACCTATGCTCGGC (21)	17	0	6.84 ± 1.32	7.0E-06
AGCATGTGCAAGTCGGGTGTG (21)	7	0	6.95 ± 0.66	3.6E-03
TTCGGCCAAGCCCTCTAGGATC (22)	6	0	6.47 ± 0.69	9.4E-03
ATGGAATCACAGTGTCTGAAC (21)	0	14	-7.78 ± 0.55	8.1E-05

Fig. 1. Characterization of durum wheat NILs differing in the presence or absence of the glaucous trait. (*A*) Phenotypes of the four NIL pairs, AG2/AG2N, AG1/AG1N, AE3/AE3N, and D051/D051N. Each pair consists of a glaucous line and a corresponding NG (N) isoline. (*B*) GC-MS analysis of the surface waxes confirms that the glaucous appearance is caused by the presence of β-diketones. (*C*) qPCR analysis of seven target genes present on chromosome 2BS including the *W1* cluster genes *W1-COE*, *W1-PKS*, and *W1-CYP*. Target genes were identified through differential expression analysis using RNA-seq (Dataset S1). (*D*) Differentially expressed sRNAs common to all four NIL comparisons described in *A*. Black sequence color indicates a perfect match to the putative *Iw1* sequence; red indicates probable sRNA U/A tailing modifications; blue-colored sRNA up-regulated in glaucous lines does not map to *Iw1*. Total read counts (Cnt) were normalized to 10 million total reads; FDR represents the highest significance of an isogenic pair; the significance threshold was at an adjusted *P* value (FDR) ≤ 0.05.

result further confirmed the hypothesis that *W1-COE* has a primary role in regulating diketone wax production in the durum NILs and is in agreement with recent reports identifying the barley *Cer-cqu* and wheat *W1* gene clusters (23, 24).

sRNAs Associated with the NG State Show Targeting Specificity for *W1-COE*. Differential expression analysis of sRNAs of 19–28 nt in length (edgeR adjusted *P* value ≤ 0.05) revealed a series of 19- to 22-nt sequences in NG lines that were almost completely absent in glaucous lines (Fig. 1*D* and Dataset S3*A*). These sRNA sequences up-regulated in NG lines could not be perfectly mapped to the IWGSC wheat genome survey sequences. However, the most abundant sRNA, 21 nt in length with 9,403 total reads and 457 average reads per 10 million (Fig. 1*D*), mapped to *W1-COE* with one mismatch (Dataset S3 *A* and *B*). From the sRNA reads, five other 19- to 22-nt sequences also mapped to *W1-COE* with one mismatch or less (Dataset S3*B*). Because the most abundant sRNA was complementary to a specific sequence in *W1-COE*, we designated the sRNA sequence as "microRNA specific to *W1-COE*" (miRW1) (Fig. 2). As mentioned, expression of miRW1 and other related sRNAs was almost absent in glaucous lines but was present in NG lines, including the F1 heterozygous progeny of crosses between the glaucous and NG NILs (Fig. 3*A* and Dataset S3 *A* and *B*). Because miRW1 had no sequence homolog other than *W1-COE* sequences in the wheat NCBI unigene set or coding sequences within the IWGSC survey sequence (Dataset S4*A*), we considered the possibility that miRW1 was derived from *W1-COE*. However, RNA structure-prediction software indicated that the *W1-COE* transcript could not fold to form a hairpin loop structure characteristic of miRNA precursors. Furthermore, the concept of *W1-COE* as a miRNA precursor is inconsistent with the inverse correlation between *W1-COE* and miRW1 expression (i.e., *W1-COE* being expressed in glaucous lines and miRW1 being preferentially expressed in NG lines). Therefore, the more likely explanation is that miRW1 is produced from an unknown precursor gene and targets *W1-COE* for suppression.

The miRW1 Precursor Contains a Hairpin-Forming Inverted Repeat with Homology to *W1-COE*. We hypothesized that the putative miRW1 precursor could have weak homology to *W1-COE* based on evidence from the literature indicating that miRNAs and their targets can have sequence similarities that extend beyond the sequence of the miRNA itself (36, 37). Because 8 of the 18 differentially expressed miRNAs had homology to *W1-COE* (with three mismatches or fewer) (Dataset S3*B*), we surmised that the NG lines may contain RNA-seq reads from a precursor sequence with homology to *W1-COE*. Thus, all RNA-seq reads from NG lines, in which the putative miRNA precursor, but not *W1-COE*, would be

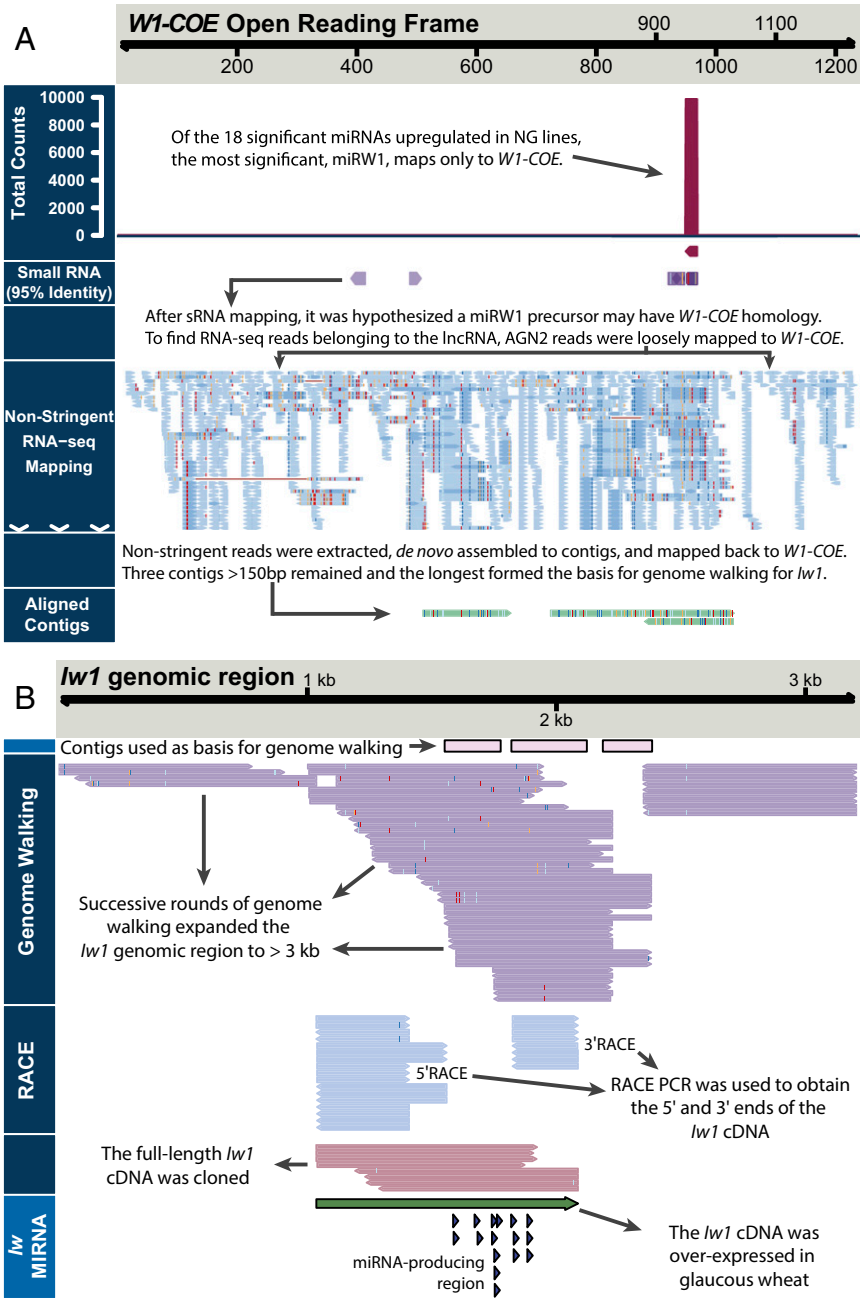

Fig. 2. Identification and cloning of *lw1* from NG durum wheat NILs. (*A*) Schematic representation of the *lw1* cloning strategy. The premise of the experiment was to identify the *lw1* sequence based on its suspected loose homology to the suspected regulatory target *W1-COE*. (*B*) After identification of potential *lw1* contigs, genome walking was performed to isolate a 3-kb genomic DNA fragment from NG NILs. Using 5′ and 3′ RACE PCR, a 1-kb cDNA was obtained that included a region where differential sRNA mapped (Fig. 1*D* and Dataset S3). Nucleotide polymorphisms within sequencing reads and contigs are represented by colored bars.

expressed were pooled and aligned against *W1-COE* with low stringency (requiring a contiguous aligned read length of >20% to *W1-COE* with >80% homology). The mapped sequences were extracted and collected for de novo assembly. Three contigs of greater than 150 nt were obtained (Fig. 2*A*). Several of the differentially expressed sRNA sequences, including the most abundant miRW1 sequence, could be perfectly mapped to two of these contigs, suggesting that one or more of the contigs was part of the miRW1 precursor (Fig. 2*B*). These contigs were the starting point for a series of genome-walking experiments that allowed us to obtain a putative 3,207-nt genomic sequence fragment (Fig. 2*B*). Because many *MIRNA* genes have a 5′ cap structure and 3′ polyadenylation (38, 39), we performed 5′ and 3′ RACE-PCR from primers designed around the location where the sRNAs mapped within the precursor fragment obtained from genome walking (Fig. 2*B* and *SI Appendix*, Table S4). Through RACE, two primary miRNA sequences differing by three bases at the 5′ end were obtained, the longest of which was 1,051 nt. Sequence analysis revealed that the miRW1 precursor is a lncRNA that contains an inverted repeat (IR) from nucleotides 520–756 and from nucleotides 770–1014 with high base-paring probability (Fig. 3*B*). Structure prediction indicated with high confidence that the lncRNA could fold into a long hairpin loop structure with the IR forming the stem (Fig. 3*C*). Analysis of the similarity between the

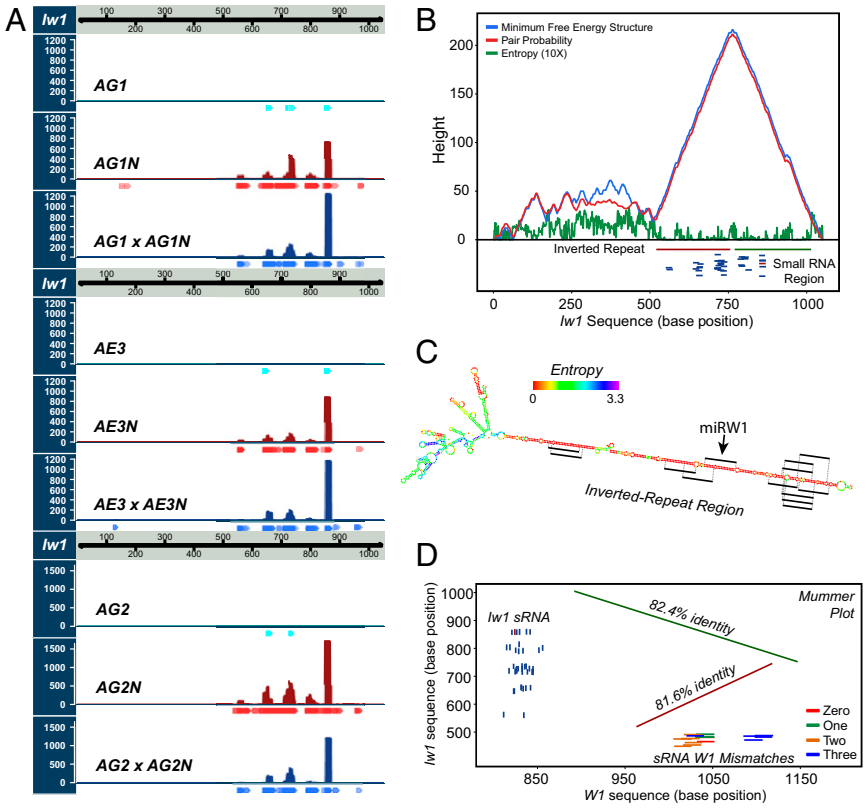

Fig. 3. Characterization of the *lw1* lncRNA. (*A*) Expression of sRNA mapping to *lw1* in three pairs of NILs and in the F1 heterozygous generation resulting from genetic crosses between each pair of isolines. (*B*) *lw1* contains an IR with high base-paring probability. The mountain plot demonstrates that the 3′ end of *lw1* (~500 bp) has a high probability of forming a hairpin structure in the region of an IR. An sRNA-producing region is identified within this hairpin IR. (*C*) The *lw1* hairpin structure. The IR region has the highest base-pairing probability consistent with low entropy values. Significant sRNAs with perfect homology are shown. (*D*) A mummer plot displays the relationship of *lw1* and its potential target gene *W1-COE*. The IR region shows greater than 80% identity with portions of the *W1* gene. sRNA mapping to *lw1* (perfect match) and to *W1-COE* (up to three mismatches) are also displayed.

lncRNA and *W1-COE* showed that each repeat of the *MIRW1* hairpin shares ~82% identity with the *W1-COE* sequence (Fig. 3*D*), suggesting that the IR of the lncRNA originated from an inverted duplication of *W1-COE*, the mechanism proposed by Allen et al. (40). Of the 18 sRNAs significantly up-regulated in NG lines, 13, including the miRW1 sequence, mapped perfectly to the foldback region of the lncRNA, and all the sRNAs up-regulated in NG lines can be mapped to the lncRNA if sRNA tailing is considered (Fig. 3*C* and Dataset S4*B*). Tailing involves the nontemplated addition of bases to the 3′ end of sRNAs through adenylation or uridylation (41–43). Taking these findings together, we conclude that the miRW1 precursor forms a long hairpin structure that is processed to produce miRW1 and other sRNAs that specifically target *W1-COE*.

Expression of the miRW1 Precursor in Glaucous Wheat Creates an NG Phenotype Through Repression of *W1-COE* and *W2-COE*. Introduction of the 1,051-nt miRW1 precursor driven by the maize ubiquitin1 promoter into the bread wheat cultivar Bobwhite resulted in an obvious NG appearance in 20 of 29 T0 plants (Fig. 4 and Dataset S5*A*). Analysis of diketone waxes in T0 transgenic lines also revealed that the NG trait was the result of the absence of β-diketones (*SI Appendix*, Fig. S5). The NG phenotype and the absence of diketone waxes was heritable and carried over to the T1 generation (*SI Appendix*, Figs. S6 and S7).

RNA-seq analyses of five NG and four glaucous T0 plants were carried out to determine both differentially expressed genes and sRNAs. Similar to the analysis of the wax NILs, we used two approaches: mapping to the NCBI unigene set and pseudoalignment to the IWGSC v1 transcript set. Four unigenes in the NG T0 lines were significantly down-regulated (edgeR adjusted P value ≤ 0.05); all were fragments of *W1-COE* or its paralog on chromosome 2DS, *W2-COE* (*SI Appendix*, Table S2). Following pseudoalignment with kallisto, the only differentially expressed transcript was *W1-COE* (DESeq2 adjusted P value ≤ 0.05) (*SI Appendix*, Table S3). Of the sRNAs, 222 were differentially up-regulated in the NG T0 lines (edgeR adjusted P value ≤ 0.05) (Dataset S5*B*), and 208 of the 222 could be mapped to the miRW1 precursor when tailing was considered (Dataset S4*C*). Other significantly up-regulated sRNAs mapped perfectly to *W1-COE* and its paralog on 2DS (*W2-COE*) (Dataset S4*D*). The numbers of sRNAs mapping to the miRW1 precursor and to the targets *W1-COE* and *W2-COE* are consistent with the observed reductions in *W1-COE* and *W2-COE* transcript levels in NG phenotypes (Fig. 4 and *SI Appendix*, Fig. S8).

To validate that *W1-COE* is the target of miRNA-guided cleavage in the transgenic lines, we performed a 5′ RACE assay to map possible cleavage sites within *W1-COE* (Fig. 5*A*). The principal position of cleavage within *W1-COE* was within the miRW1-binding site located between nucleotides 10 and 11 and was present in 14 of 15 cloned sequences. Furthermore, in NG transgenic lines with active cleavage of *W1-COE*, we detected the presence of secondary siRNA in the 3′ cleavage fragment (Fig. 5*B*). The majority of these siRNAs were 21 nt in length and were positively related to both the abundance of miRW1 and its monouridylated form (*SI Appendix*, Fig. S9 *A* and *B*). Secondary siRNAs also were apparent in the 3′ region adjacent to the miRW1-binding site in *W2-COE* (*SI Appendix*, Fig. S9*C*). The presence of secondary siRNAs also was detected in the heterozygous

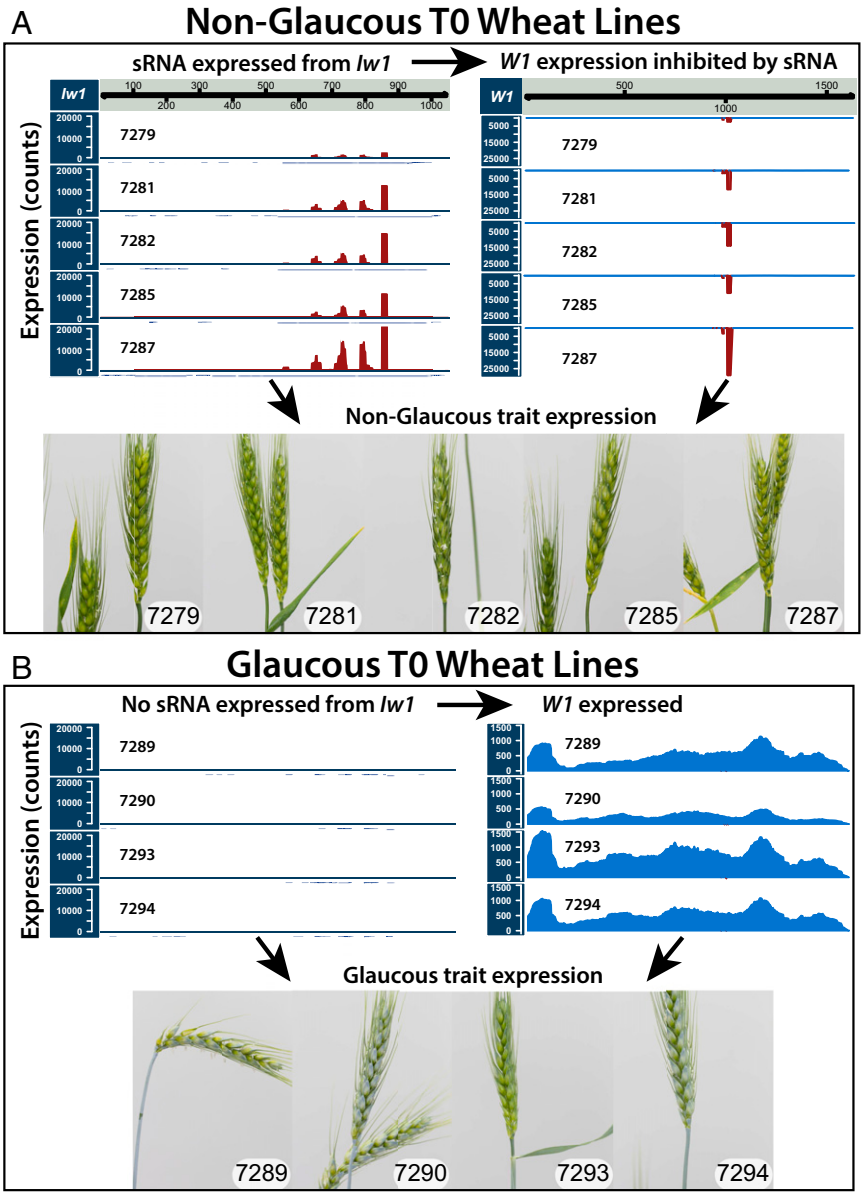

Fig. 4. Characterization of transgenic lines overexpressing *Iw1* through sRNA and RNA-seq analyses. (*A*) NG T0 overexpression lines displaying expression of sRNA derived from *Iw1* and repression of *W1-COE*. (*B*) In contrast, glaucous T0 lines showed almost no expression of sRNA from *Iw1* and showed expression of *W1-COE*. Analyses of sRNA and RNA-seq data demonstrated that the differences between the glaucous and NG lines were caused by the expression of sRNA from *Iw1* and the resulting repression of *W1-COE* (*SI Appendix*, Tables S2 and S3 and Dataset S5). GC-MS experiments in the T0/T1 generation confirmed that the NG trait was caused by the absence of β-diketones (*SI Appendix*, Figs. S5–S7).

F1 generation in the isogenic lines but, interestingly, not in the NG homozygous lines (*SI Appendix*, Fig. S9*D*).

These results from the introduction of the miRW1 precursor into glaucous wheat provide further validation that miRW1 acts as a repressor of wax production through miRNA-mediated suppression of *W1-COE*/*W2-COE* expression. The results from the overexpression experiments suggest that the miRW1 precursor is the wax inhibitor *Iw1*, the expression of which has the ability to silence specifically both *W1-COE* and *W2-COE*.

The IR Region of *Iw1* Maps to the Location of *Iw2*. We were unable to map the *Iw1* sequence to the IWGSC wheat genome survey sequences, indicating that *Iw1* is not represented in the currently available reference genomes for the Chinese Spring cultivar. However, a 689-nt *Iw1* fragment was mapped to scaffold 10812 of chromosome 2 of the D genome progenitor *Ae. tauschii* (44). Further, this *Iw1* fragment maps to the precise location in *Ae. tauschii* to which *Iw2* has been fine mapped previously (12) (Fig. 6*A* and *SI Appendix*, Fig. S10), and the location is consistent with genetic markers from syntenic blocks from species such as *Brachypodium distachyon* that include the genes *BRADI5G01180* and *BRADI5G01160* (17, 18, 44). The *Iw1* homology region lies within the promoter region of the *Ae. tauschii* gene F775_09277 encoding cytochrome P450 84A1 (Fig. 6*A*). Additional mapping evidence comes from the synthetic hexaploid wheat W7984, for which a shotgun survey sequence assembly is available (45). Comparative analysis of the collinear regions of *Ae. tauschii* and W7984 revealed that the *Iw1* fragment maps to W7984 scaffold 212941 in a similar context as in *Ae. tauschii* (Fig. 6*B* and *SI Appendix*, Fig. S10). Therefore, based on the dominant-negative effect of *Iw1* and miRW1 on the glaucous trait and the colocalization of an *Iw1* fragment with markers for

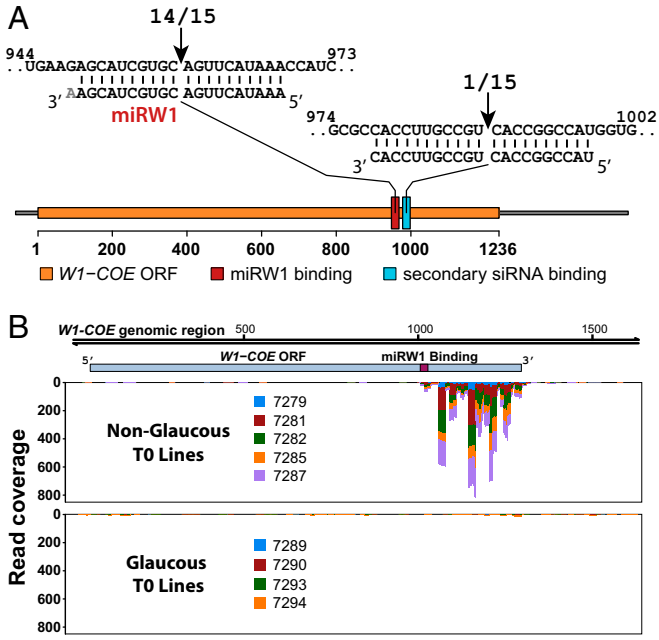

Fig. 5. Validation of the cleavage of the *W1-COE* mRNA target by miRW1. (*A*) *W1-COE* cleavage sites identified by 5′ RACE. Sequences of 14 of 15 clones showed cleavage between nucleotides 10 and 11 of the miRW1-binding site. One cleavage site was located within a minor sRNA-binding site between the 10th and 11th nucleotide. (*B*) Mapping of secondary siRNAs to *W1-COE* in *Iw1* T0 transgenic lines. (*Upper*) sRNAs with perfect homology to *W1-COE* mapped to a region 3′ of the miRW1-binding site in NG lines. (*Lower*) Almost none did so in glaucous lines.

Iw2, we propose that two miRW1 precursors, *Iw1* and *Iw2*, are present on chromosomes 2BS and 2DS, respectively. The IR and sRNA-producing regions of *Iw1* and *Iw2* are highly homologous (94%), and both are energetically favored to form a hairpin structure (Fig. 6*C*). Additional evidence of an *Iw2* hairpin-forming RNA comes from sRNA sequencing experiments downloaded at the NCBI short-read archive from Li et al. (46). Similar to *Iw1*, the *Iw2* region also produces a series of sRNAs, including the most dominant sequence miRW1 (Fig. 6*D*).

Discussion

We have identified and validated the regulatory function of *Iw1* and confirmed the role of a key gene, *W1-COE*, within the *W1* locus. *Iw1* and its homolog *Iw2* are young MIRNA genes with long hairpin precursors which ultimately suppress β-diketone wax production. *Iw1* and *Iw2* produce miRW1, which specifically targets and represses the expression of the putative carboxylesterase genes that are necessary for the production of β-diketone waxes in wheat (24). Identification of the *Iw* loci represents a major step forward in our regulatory understanding of the glaucous trait in wheat and related species, from both a functional and an evolutionary standpoint.

miRNAs have a significant regulatory role in plants and target a wide range of transcripts for degradation and therefore are inherently dominant-negative genetic factors (28, 41). Many evolutionarily conserved miRNA families play critical roles in plant development and adaptation to diverse environments. There also are many nonconserved, evolutionarily recent miRNAs and their corresponding targets that are present only within a few closely related species or appear to be unique to specific species (47–49). Wheat miRNA sequencing, identification, profiling, and characterization have been reported extensively (50–56). However, neither miRW1 nor its precursor has been reported, possibly because of the atypical characteristics of *Iw1* and *Iw2*. In fact, the *Iw1* sequence does not exist in any available wheat genome reference or sequencing database such as the NCBI. The identification of *Iw1* and *Iw2* as long noncoding, hairpin-forming, sRNA-producing RNAs with IRs similar to their target sequence places them among the few functional lncRNAs described in monocots, the most notable previous example being the maize *Mu killer* locus (57). *Mu killer* arose from an inverted duplication of a sequence similar to its target, the MuDR transposon; however *Mu killer* acts via the production of siRNAs and an epigenetic mechanism (58, 59) instead of the miRNA-based silencing mechanism of the *Iw* genes. lncRNA-mediated gene regulation is emerging as a common regulatory mechanism in plants. A variety of lncRNA-mediated regulation mechanisms have been unraveled, including target mimicry, transcription interference, PRC2-associated histone methylation, and DNA methylation (26). However, although the number of known plant lncRNAs is expanding, the great majority have no known function (60–65). In wheat, the lncRNA landscape has been profiled during fungal responses and heat stress, but the characterization of function is deficient (66, 67).

As described here, *Iw1* and *Iw2* serve as miRNA precursors and repress target gene expression through a miRNA-mediated mechanism. Several lines of evidence indicate that *Iw1* and *Iw2* are evolutionarily young MIRNA genes that arose by inverted duplication of their target gene (39, 49). First, the foldback region of *Iw1* has extended similarity (>80%) with the target *W1-COE* beyond that of the miRW1 region. Second, the *Iw1* primary transcript (1,051 nt) is much longer than typical miRNA primary sequences; 98% of miRNA precursor lengths are <336 nt with a mean of 146 nt (68). Third, the foldback regions of *Iw1* and *Iw2* are hairpin structures >200 nt that resemble a dsRNA and do not resemble the typical short structure of miRNA hairpins. In *Arabidopsis*, Ben Amor et al. (27) identified nine ncRNAs corresponding to miRNA, *trans*-acting siRNA, and 24-nt siRNA precursors, including a young MIRNA gene *MIR869A*. The transcript of *MIR869A* is processed by DCL4, because its secondary structure is closer to that of dsRNA than to that of a typical, short miRNA precursor processed by DCL1 (69). The example of *MIR869a* might indicate the evolutionary path of the *Iw* genes, with younger dsRNA-forming MIRNA genes evolving through the production of miRNA-like siRNA, because the *Iw1* and *Iw2* hairpin precursors also produce other sRNAs in addition to the predominant 21-nt miRW1. Fourth, we show evidence that miRW1, the predominant miRNA, is primarily responsible for the cleavage of the *W1-COE* transcript. Moreover, cleavage between nucleotides 10 and 11 of miRW1 is consistent with the principle hallmark of miRNA-guided degradation (40, 70, 71). The presence of secondary siRNAs mapping to the 3′ cleavage fragment in the NG *Iw1* overexpression and F1 heterozygous crosses of NIL pairs provides additional evidence of miRNA-directed degradation of *W1-COE* and *W2-COE*. In plants there are two models, "one-hit" and "two-hit," for secondary siRNA production. In the one-hit model, the trigger can be binding of 22-nt miRNAs, and in the two-hit model the trigger can be two neighboring miRNA target sites on the same mRNA (72, 73). Both models are possible triggers for the secondary siRNAs arising from the cleavage of *W1-COE* (and *W2-COE*). A 22-nt monouridylated form of miRW1 supports the one-hit model; alternatively, additional miRNAs arising from *Iw1* with *W1-COE* as a potential binding target support the two-hit model. As mentioned above, one curious aspect of the discovery of secondary siRNA arising from *W1-COE* is the absence of secondary siRNA in the homozygous NILs, and this difference leads into a discussion of whether *W1* genes are present in NG lines and cultivars.

One feature of the results leading to the identification of *W1* and *Iw1* is that in homozygous NG NILs other genes in addition to *W1-COE* are strongly down-regulated (Fig. 1*C*), notably *W1-PKS* and *W1-CYP* in the *W1* gene cluster on chromosome 2BS, which

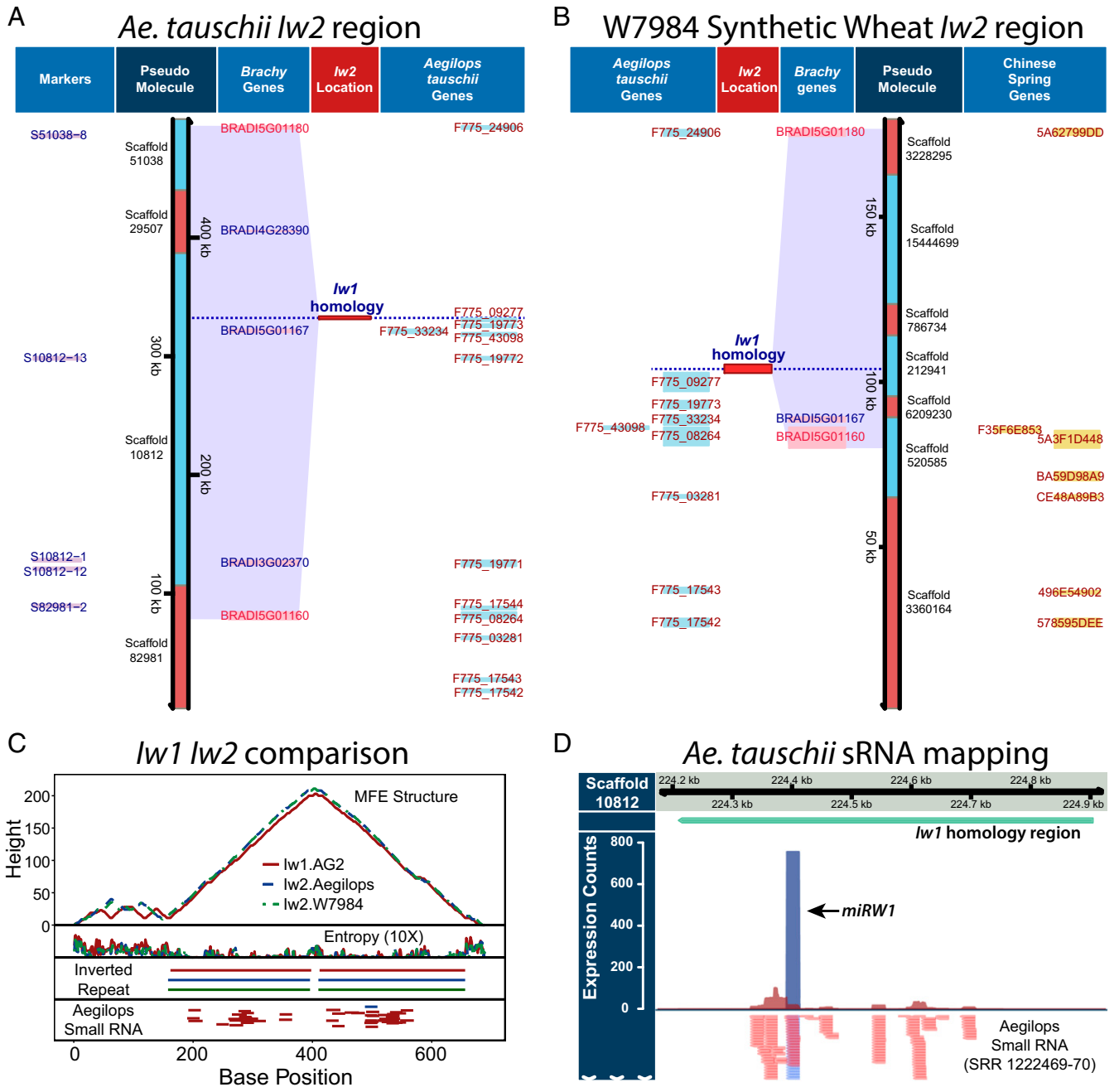

Fig. 6. *Iw2* in the D subgenome is a paralog of *Iw1* from the B subgenome. (*A* and *B*) The IR, sRNA-producing sequence of *Iw1* maps to the *Iw2* region in *Ae. tauschii* and the W7984 synthetic hexaploid wheat (SHW). The location of the *Iw1* homology region is consistent with *Ae. tauschii* S10812 markers and the *Brachypodium distachyon* (Brachy) genes *BRADI5G01180* and *BRADI5G01160*. (*C*) Comparison of *Iw1* and the homologous *Ae. tauschii* and W7984 SHW sequences reveals a high similarity including ~95% sequence identity between *Iw1* and the D-genome sequences, the presence of IRs, and high base-pairing probabilities in the minimum free energy (MFE) structure. (*D*) sRNA libraries from spikes of *Ae. tauschii* revealed a similar pattern of sRNAs in the 689-bp *Iw1* homology region on *Ae. tauschii* scaffold 10812 with the 21-bp sequence miRW1 predominating.

also are involved in the β-diketone and OH-β-diketone synthesis pathways (24). However, *Iw1* dominantly regulates glaucousness through miRW1-promoted cleavage and mRNA degradation of *W1-COE*, and overexpression of *Iw1* in bread wheat down-regulated only *W1-COE* and its paralog *W2-COE* (Fig. 4 and *SI Appendix*, Tables S2 and S3). Moreover, in NG F1 heterozygous lines, which manifest *Iw1* dominance, *W1-COE* was the key down-regulated gene related to diketone wax synthesis (Fig. 1*C*). These results show, first, that *Iw1*-mediated repression of *W1-COE* causes loss of the glaucous phenotype and, second, that there is another mechanism that down-regulates multiple genes at the *W1* locus in NG homozygotes. Interestingly, Hen-Avivi et al. (24) provide evidence that *W1-COE*, *W1-PKS*, and *W1-CYP* are missing from the *W1*/*Iw1* genomic interval in the glossy, *Iw1*-containing wild emmer accession TTD140 but are present in the *W1* metabolic gene cluster found in the glaucous cultivar Zavitan. The idea that the *W1* genes are missing or have moved to a transcriptionally inactive part of the genome in the NG genotype is interesting and is consistent with our observations of very strong down-regulation of the W1 cluster and the lack of secondary siRNAs from *W1-COE*

in the homozygous NILS. However, the relationship between the *W1* gene cluster and *Iw* needs to be explored further by sequencing more glaucous and NG cultivars.

The presence of *Iw* in selected species within the Triticeae tribe allows us to propose an approximate evolutionary origin of *Iw*. Barley, which contains diketone wax but in which there are no reports of a dominant wax inhibitor gene, diverged from wheat 8–12 Mya, suggesting that the inverted duplication event that created *Iw* occurred after this date (74–77). The inverted duplication may have been a single event in an ancestral wheat genome lineage or separate later events resulting in convergent evolution in B (*Iw1*) and D (*Iw2*) genome species. A single inverted duplication of *W1-COE* in an ancestral B genome is plausible, based on the evidence presented by Marcussen et al. (15), who suggest that a hybridization event between A and B lineages occurred ∼5.5 Mya and led to the origin of the D genome lineage. The time of *Iw* creation at <12 Mya is comparable to the creation of young MIRNA genes in the *Arabidopsis* genus at <20 Mya or in *Arabidopsis thaliana* itself at <10 Mya (49, 78–81). In contrast, more ancient conserved MIRNA genes (e.g., miR156) predate the separation of the monocots and dicots at ∼150 Mya (82).

In summary, the specific and unique interaction between *Iw* and miRW1 with *W-COE* represents a mechanism for dominant gene repression and provides a basis for genome-wide identification of other nonconserved lncRNA functions or atypical MIRNA genes. Furthermore, the identification of the *Iw* genes as a major regulatory mechanism governing *W-COE* expression and β-diketone deposition suggests the possibility of precise gene editing or marker-based manipulation of glaucousness for better adaptation to specific conditions and environments.

Materials and Methods

Details of sample preparation, experimental procedures, and data analysis with associated references can be found in *SI Appendix, Materials and Methods*.

The sRNA and RNA-seq data have been submitted to the Sequence Read Archive (SRA) at the NCBI with the accession numbers SAMN05725181–SAMN05725246 (mRNAs and sRNAs in *Triticum durum* and *Triticum aestivum*). The *Iw1* full-length cDNA sequence was submitted to dbEST (NCBI). The accession number is KX823910.

ACKNOWLEDGMENTS. We thank Drs. Jitao Zou of the National Research Council of Canada (NRC), Andrew Sharpe (Global Institute for Food Security, University of Saskatchewan), and Weiren Wu (Fujian Agriculture and Forestry University) for helpful comments during the course of the project and in the preparation of this paper; Dr. Ron Knox (Agriculture and Agri-Food Canada) for providing the NILs used in this research; Mr. Joe Hammerlindl and Mr. Allan Kolenovsky of the NRC-Saskatoon Plant Transformation Service Facility for wheat transformation and selection of transformants; Dr. Shawn Clark and Mr. Enwu Liu for suggestions regarding VIGS experiments; Mr. Darwin Reed for optimizing GC-MS conditions for wax analyses and for locating wax standards synthesized by the late Dr. Pat Tulloch and colleagues; the NRC-Saskatoon Genomics Service Facility for DNA, RNA, and sRNA sequencing; Mr. Dustin Cram for bioinformatics assistance; and Drs. Assaf Distelfeld (Tel-Aviv University) and Cristobal Uauy (John Innes Centre) for providing access to additional genome sequence data. Funding for this project was provided by the NRC through the Canadian Wheat Alliance. This paper is NRCC No. 56262.

1. Shepherd T, Wynne Griffiths D (2006) The effects of stress on plant cuticular waxes. *New Phytol* 171:469–499.
2. Von Wettstein-Knowles P (2012) *Plant Waxes* (John Wiley & Sons, Ltd, Chichester, UK).
3. Zhang Z, Wang W, Li W (2013) Genetic interactions underlying the biosynthesis and inhibition of β-diketones in wheat and their impact on glaucousness and cuticle permeability. *PLoS One* 8:e54129.
4. Wang Y, et al. (2015) Developmental changes in composition and morphology of cuticular waxes on leaves and spikes of glossy and glaucous wheat (*Triticum aestivum* L.). *PLoS One* 10:e0141239.
5. Tulloch AP, Baum BR, Hoffman LL (1980) A survey of epicuticular waxes among genera of *Triticeae*. 2. Chemistry. *Can J Bot* 58:2602–2615.
6. Clarke JM, McCaig TN, DePauw RM (1993) Relationship of glaucousness and epicuticular wax quantity of wheat. *Can J Plant Sci* 73:961–967.
7. Johnson DA, Richards RA, Turner NC (1983) Yield, water relations, gas exchange, and surface reflectance of near-isogenic lines differing in glaucousness. *Crop Sci* 23: 318–325.
8. Richards RA, Rawson HM, Johnson DA (1986) Glaucousness in wheat: Its development and effect on water-use efficiency, gas exchange and photosynthetic tissue temperature. *Aust J Plant Physiol* 13:465–473.
9. Monneveux P, et al. (2004) Relationships between grain yield, flag leaf morphology, carbon isotope discrimination and ash content in irrigated wheat. *J Agron Crop Sci* 190:395–401.
10. Tsunewaki K (1966) Comparative gene analysis of common wheat and its ancestral species. II. Waxiness, growth habit and awnedness. *Jpn J Bot* 19:175–254.
11. Xu Z, Yuan C, Wang J, Fu D, Wu J (2015) Mapping the glaucousness suppressor *Iw1* from wild emmer wheat 'PI 481521'. *Crop J* 3:37–45.
12. Nishijima R, Iehisa JCM, Matsuoka Y, Takumi S (2014) The cuticular wax inhibitor locus *Iw2* in wild diploid wheat *Aegilops tauschii*: Phenotypic survey, genetic analysis, and implications for the evolution of common wheat. *BMC Plant Biol* 14:246.
13. Simmonds JR, et al. (2008) Mapping of a gene (*Vir*) for a non-glaucous, viridescent phenotype in bread wheat derived from *Triticum dicoccoides*, and its association with yield variation. *Euphytica* 159:333–341.
14. Liu Q, et al. (2007) Molecular mapping of a dominant non-glaucousness gene from synthetic hexaploid wheat (*Triticum aestivum* L). *Euphytica* 155:71–78.
15. Marcussen T, et al.; International Wheat Genome Sequencing Consortium (2014) Ancient hybridizations among the ancestral genomes of bread wheat. *Science* 345: 1250092.
16. Tsunewaki K, Ebana K (1999) Production of near-isogenic lines of common wheat for glaucousness and genetic basis of this trait clarified by their use. *Genes Genet Syst* 74: 33–41.
17. Adamski NM, et al. (2013) The *inhibitor of wax 1* locus (*Iw1*) prevents formation of β- and OH-β-diketones in wheat cuticular waxes and maps to a sub-cM interval on chromosome arm 2BS. *Plant J* 74:989–1002.
18. Wu H, et al. (2013) Comparative high-resolution mapping of the wax inhibitors *Iw1* and *Iw2* in hexaploid wheat. *PLoS One* 8:e84691.
19. Lu P, et al. (2015) Comparative fine mapping of the *Wax 1* (*W1*) locus in hexaploid wheat. *Theor Appl Genet* 128:1595–1603.
20. von Wettstein-Knowles P, Søgaard B (1980) The *cer-cqu* region in barley: Gene cluster or multifunctional gene. *Carlsberg Res Commun* 45:125–141.
21. von Wettstein-Knowles P (1995) Biosynthesis and genetics of waxes. *Waxes: Chemistry, Molecular Biology and Functions*, ed RJ Hamilton (Oily, Allowry, Ayr, Scotland), pp 91–130.
22. Anonymous (1996) Description of *glossy sheath 1*. *Barley Genet Newsl* 26:292.
23. Schneider LM, et al. (2016) The Cer-cqu gene cluster determines three key players in a β-diketone synthase polyketide pathway synthesizing aliphatics in epicuticular waxes. *J Exp Bot* 67:2715–2730.
24. Hen-Avivi S, et al. (2016) A metabolic gene cluster in the wheat W1 and the barley Cer-cqu loci determines β-diketone biosynthesis and glaucousness. *Plant Cell* 28: 1440–1460.
25. Iyer MK, et al. (2015) The landscape of long noncoding RNAs in the human transcriptome. *Nat Genet* 47:199–208.
26. Zhang J, Mujahid H, Hou Y, Nallamilli BR, Peng Z (2013) Plant long ncRNAs: A new frontier for gene regulatory control. *Am J Plant Sci* 4:1038–1045.
27. Ben Amor B, et al. (2009) Novel long non-protein coding RNAs involved in *Arabidopsis* differentiation and stress responses. *Genome Res* 19:57–69.
28. Ghildiyal M, Zamore PD (2009) Small silencing RNAs: An expanding universe. *Nat Rev Genet* 10:94–108.
29. Bartel DP (2009) MicroRNAs: Target recognition and regulatory functions. *Cell* 136: 215–233.
30. Clarke JM, McCaig TN, DePauw RM (1994) Inheritance of glaucousness and epicuticular wax in durum wheat. *Crop Sci* 34:327–330.
31. Clarke JM, et al. (1995) Registration of seven pairs of durum wheat genetic stocks near-isogenic for glaucousness. *Crop Sci* 35:1241.
32. Bianchi G, Figini ML (1986) Epicuticular waxes of glaucous and nonglaucous durum wheat lines. *J Agric Food Chem* 34:429–433.
33. Bray NL, Pimentel H, Melsted P, Pachter L (2016) Near-optimal probabilistic RNA-seq quantification. *Nat Biotechnol* 34:525–527.
34. Love MI, Huber W, Anders S (2014) Moderated estimation of fold change and dispersion for RNA-seq data with DESeq2. *Genome Biol* 15:550.
35. Yuan C, et al. (2011) A high throughput barley stripe mosaic virus vector for virus induced gene silencing in monocots and dicots. *PLoS One* 6:e26468.
36. Axtell MJ, Bowman JL (2008) Evolution of plant microRNAs and their targets. *Trends Plant Sci* 13:343–349.
37. Nozawa M, Miura S, Nei M (2012) Origins and evolution of microRNA genes in plant species. *Genome Biol Evol* 4:230–239.
38. Xie Z, et al. (2005) Expression of Arabidopsis MIRNA genes. *Plant Physiol* 138: 2145–2154.
39. Bologna NG, et al. (2013) Multiple RNA recognition patterns during microRNA biogenesis in plants. *Genome Res* 23:1675–1689.
40. Allen E, et al. (2004) Evolution of microRNA genes by inverted duplication of target gene sequences in *Arabidopsis thaliana*. *Nat Genet* 36:1282–1290.
41. Borges F, Martienssen RA (2015) The expanding world of small RNAs in plants. *Nat Rev Mol Cell Biol* 16:727–741.
42. Chou MT, et al. (2015) Tailor: A computational framework for detecting non-templated tailing of small silencing RNAs. *Nucleic Acids Res* 43:e109.
43. Zhai J, et al. (2013) Plant microRNAs display differential 3′ truncation and tailing modifications that are ARGONAUTE1 dependent and conserved across species. *Plant Cell* 25:2417–2428.

44. Jia J, et al.; International Wheat Genome Sequencing Consortium (2013) *Aegilops tauschii* draft genome sequence reveals a gene repertoire for wheat adaptation. *Nature* 496:91–95.
45. Chapman JA, et al. (2015) A whole-genome shotgun approach for assembling and anchoring the hexaploid bread wheat genome. *Genome Biol* 16:26.
46. Li A, et al. (2014) mRNA and small RNA transcriptomes reveal insights into dynamic homoeolog regulation of allopolyploid heterosis in nascent hexaploid wheat. *Plant Cell* 26:1878–1900.
47. Cuperus JT, Fahlgren N, Carrington JC (2011) Evolution and functional diversification of MIRNA genes. *Plant Cell* 23:431–442.
48. Taylor RS, Tarver JE, Hiscock SJ, Donoghue PC (2014) Evolutionary history of plant microRNAs. *Trends Plant Sci* 19:175–182.
49. Fahlgren N, et al. (2010) MicroRNA gene evolution in *Arabidopsis lyrata* and *Arabidopsis thaliana*. *Plant Cell* 22:1074–1089.
50. Sun F, et al. (2014) Whole-genome discovery of miRNAs and their targets in wheat (*Triticum aestivum* L.). *BMC Plant Biol* 14:142.
51. Pandey R, Joshi G, Bhardwaj AR, Agarwal M, Katiyar-Agarwal S (2014) A comprehensive genome-wide study on tissue-specific and abiotic stress-specific miRNAs in *Triticum aestivum*. *PLoS One* 9:e95800.
52. Han R, et al. (2014) Identification and characterization of microRNAs in the flag leaf and developing seed of wheat (*Triticum aestivum* L.). *BMC Genomics* 15:289.
53. Budak H, Khan Z, Kantar M (2015) History and current status of wheat miRNAs using next-generation sequencing and their roles in development and stress. *Brief Funct Genomics* 14:189–98.
54. Yao Y, Sun Q (2012) Exploration of small non coding RNAs in wheat (*Triticum aestivum* L.). *Plant Mol Biol* 80:67–73.
55. Meng F, et al. (2013) Development-associated microRNAs in grains of wheat (*Triticum aestivum* L.). *BMC Plant Biol* 13:140.
56. Agharbaoui Z, et al. (2015) An integrative approach to identify hexaploid wheat miRNAome associated with development and tolerance to abiotic stress. *BMC Genomics* 16:339.
57. Slotkin RK, Freeling M, Lisch D (2003) *Mu killer* causes the heritable inactivation of the Mutator family of transposable elements in *Zea mays*. *Genetics* 165:781–797.
58. Slotkin RK, Freeling M, Lisch D (2005) Heritable transposon silencing initiated by a naturally occurring transposon inverted duplication. *Nat Genet* 37:641–644.
59. Tricker PJ (2015) Transgenerational inheritance or resetting of stress-induced epigenetic modifications: Two sides of the same coin. *Front Plant Sci* 6:699.
60. Bazin J, Bailey-Serres J (2015) Emerging roles of long non-coding RNA in root developmental plasticity and regulation of phosphate homeostasis. *Front Plant Sci* 6: 400.
61. Heo JB, Lee YS, Sung S (2013) Epigenetic regulation by long noncoding RNAs in plants. *Chromosome Res* 21:685–693.
62. Wang H, et al. (2015) Analysis of non-coding transcriptome in rice and maize uncovers roles of conserved lncRNAs associated with agriculture traits. *Plant J* 84:404–416.
63. Zhang YC, et al. (2014) Genome-wide screening and functional analysis identify a large number of long noncoding RNAs involved in the sexual reproduction of rice. *Genome Biol* 15:512.
64. Li L, et al. (2014) Genome-wide discovery and characterization of maize long noncoding RNAs. *Genome Biol* 15:R40.
65. Wang H, et al. (2014) Genome-wide identification of long noncoding natural antisense transcripts and their responses to light in *Arabidopsis*. *Genome Res* 24:444–453.
66. Xin M, et al. (2011) Identification and characterization of wheat long non-protein coding RNAs responsive to powdery mildew infection and heat stress by using microarray analysis and SBS sequencing. *BMC Plant Biol* 11:61.
67. Zhang H, et al. (2016) Genome-wide identification and functional prediction of novel and fungi-responsive lincRNAs in *Triticum aestivum*. *BMC Genomics* 17:238.
68. Thakur V, et al. (2011) Characterization of statistical features for plant microRNA prediction. *BMC Genomics* 12:108.
69. Rajagopalan R, Vaucheret H, Trejo J, Bartel DP (2006) A diverse and evolutionarily fluid set of microRNAs in *Arabidopsis thaliana*. *Genes Dev* 20:3407–3425.
70. Kasschau KD, et al. (2003) P1/HC-Pro, a viral suppressor of RNA silencing, interferes with Arabidopsis development and miRNA unction. *Dev Cell* 4:205–217.
71. Huntzinger E, Izaurralde E (2011) Gene silencing by microRNAs: Contributions of translational repression and mRNA decay. *Nat Rev Genet* 12:99–110.
72. Axtell MJ, Jan C, Rajagopalan R, Bartel DP (2006) A two-hit trigger for siRNA biogenesis in plants. *Cell* 127:565–577.
73. Chen HM, et al. (2010) 22-Nucleotide RNAs trigger secondary siRNA biogenesis in plants. *Proc Natl Acad Sci USA* 107:15269–15274.
74. Huang S, et al. (2002) Phylogenetic analysis of the acetyl-CoA carboxylase and 3-phosphoglycerate kinase loci in wheat and other grasses. *Plant Mol Biol* 48:805–820.
75. Dvorak J, Akhunov ED (2005) Tempos of gene locus deletions and duplications and their relationship to recombination rate during diploid and polyploid evolution in the Aegilops-Triticum alliance. *Genetics* 171:323–332.
76. Chalupska D, et al. (2008) Acc homoeoloci and the evolution of wheat genomes. *Proc Natl Acad Sci USA* 105:9691–9696.
77. Middleton CP, et al. (2014) Sequencing of chloroplast genomes from wheat, barley, rye and their relatives provides a detailed insight into the evolution of the Triticeae tribe. *PLoS One* 9:e85761.
78. Koch MA, Haubold B, Mitchell-Olds T (2000) Comparative evolutionary analysis of chalcone synthase and alcohol dehydrogenase loci in *Arabidopsis, Arabis*, and related genera (Brassicaceae). *Mol Biol Evol* 17:1483–1498.
79. Wright SI, Lauga B, Charlesworth D (2002) Rates and patterns of molecular evolution in inbred and outbred *Arabidopsis*. *Mol Biol Evol* 19:1407–1420.
80. Ossowski S, et al. (2010) The rate and molecular spectrum of spontaneous mutations in Arabidopsis thaliana. *Science* 327:92–94.
81. Smith LM, et al. (2015) Rapid divergence and high diversity of miRNAs and miRNA targets in the Camelineae. *Plant J* 81:597–610.
82. Floyd SK, Bowman JL (2004) Gene regulation: Ancient microRNA target sequences in plants. *Nature* 428:485–486.